water

MDPI

Article

Using Sawdust Derived Biochar as a Novel 3D Particle Electrode for Micropollutants Degradation

Athanasia Petala [1,2], Georgios Bampos [1,3] and Zacharias Frontistis [1,*]

[1] Department of Chemical Engineering, University of Western Macedonia, Bakola & Sialvera, GR-50132 Kozani, Greece; natpetala@chemeng.upatras.gr (A.P.); geoba@chemeng.upatras.gr (G.B.)
[2] Department of Environment, Ionian University, GR-29100 Zakynthos, Greece
[3] Department of Chemical Engineering, University of Patras, GR-26504 Patras, Greece
* Correspondence: zfrontistis@uowm.gr

Abstract: This work examined the use of a 3D combined electrochemical process based on particle electrodes from sawdust-derived biochar pyrolized at T = 550–850 °C to remove persistent pollutants. The as-prepared biochar was characterized by scanning electron microscopy with an X-ray energy dispersive spectrometer (SEM/EDS), nitrogen adsorption (BET method) and X-ray diffraction (XRD) techniques. The use of sawdust biochar pyrolized at 650 °C led to a significant increase in efficiency against the sum of conventional 2D electrochemical systems and adsorption, and the synergy index estimated equal to 74.5% at optimum conditions. Sulfamethoxazole (SMX) removal was favored by increasing particle electrode loading. Despite that, the reaction was slightly favored in near-neutral conditions; the system retained most of its activity in the pH range 3–10. The proposed 3D system could degrade different micropollutants, namely SMX, Bisphenol A (BPA), Propylparaben (PP), and Piroxicam (PR). Of particular interest was that no significant reduction in degradation was observed in the case of complex or real water matrices. In addition, the system retained its efficiency regarding SMX removal after five sequential experiments in the 3D combined electrochemical process. However, further investigation is needed to estimate the contribution of the different mechanisms of micropollutant removal in the proposed system.

Keywords: three-dimensional electrochemical process; novel particle electrode; biochar; micropollutants; synergy

Citation: Petala, A.; Bampos, G.; Frontistis, Z. Using Sawdust Derived Biochar as a Novel 3D Particle Electrode for Micropollutants Degradation. *Water* **2022**, *14*, 357. https://doi.org/10.3390/w14030357

Academic Editor: Gopal Achari

Received: 9 December 2021
Accepted: 24 January 2022
Published: 26 January 2022

1. Introduction

Advanced oxidation processes (AOPs) have gained great interest in the last decades amongst water treatment technologies [1,2]. Their popularity derives from the fact that they successfully cover the inefficiency of conventional water treatment methods regarding the complete degradation of emerging contaminants (ECs) in water [3]. The term ECs refers to pharmaceuticals, personal care products (PPCPs), and other natural or chemical substances that have been detected at very low concentrations (in the range of μg/L or ng/L) not only in the secondary effluent of wastewater treatment plants but also at surface or ground waters. Their presence has been linked to a series of undesired effects on humans and aquatic life, such as antimicrobial resistance and risks to reproductive health [4].

The high efficiency of AOPs derives from the high oxidative power of hydroxyl radicals (•OH) generated in situ and can react with organic pollutants, leading to their complete mineralization [1,2]. Some AOPs, such as photocatalysis, are based on light for •OH production, while others are based on the addition of oxidants, such as persulfate or hydrogen peroxide [5]. Another group of AOPs proposed for wastewater treatment includes directly or indirectly electrooxidation of water on an anode surface and is known as electrochemical AOPs (EAOPs) [6].

A typical two-dimensional (2D) EAOP system consists of anode and cathode electrodes and the electrolyte [7]. Between different materials, Boron-doped diamond (BDD) electrodes

have shown very promising results as anode materials, exhibiting high stability, a large potential window, and a long lifetime [8]. For example, the removal of Procion Red MX-5B was investigated using the BDD electrode, showing complete degradation when applying low current densities [9]. Furthermore, Ti_4O_7 was very recently introduced as anode material for paracetamol degradation, showing high efficiency [10].

Electrochemical oxidation is environmentally friendly, as the main oxidant involved is the electron and not a chemical reagent. It has high efficiency; it can be automated and easily adjusted while reactions take place under mild conditions (ambient temperature and pressure), thus keeping the cost of the whole process low. Finally, the coupling with renewable energy sources for current supply can lead to a complete "green" solution to the problem of wastewater treatment [11,12].

However, one of the 2D EAOP system's main drawbacks is the small electrode surface area and mass transfer limitations [13,14]. Trying to deal with these restrictions, it was found that the addition of granular activated carbon (GAC) into the electrolyte of a 2D system could significantly enhance the reported efficiency, as, under the imposition of suitable current, these particles transform to charged microelectrodes, acting as independent electrolytic cells [15]. The increase of the electrode surface area triggers an increase in active sites for micropollutant degradation that, in combination with the increase of electrolyte conductivity and the decrease of mass transfer, greatly enhances the efficiency of the process [16,17]. In addition, the adsorption efficiency of particle electrodes was found to enhance pollutant degradation, thus making the specific surface area a determining factor for the selection of such electrodes [18].

Considering the above-mentioned requirements—a particle electrode must-have—many carbonaceous materials were firstly introduced as particle electrodes in 3D EAOP systems. Zhan et al. treated real pharmaceutical wastewaters in a 3D EAOP system using GAC as the particle electrode [19]. They also combined this process with ozonation in order to accelerate pharmaceutical removal. They showed the existence of synergistic phenomena in the combined process, resulting in a higher total organic carbon (TOC) removal than the individual processes or the equivalent 2D process. Multiwalled carbon nanotubes (MWCNTs) were used by Mengelizadeh et al. in their 3D EAOP system for Reactive Black 5 (RB5) degradation, resulting in higher $^{\bullet}OH$ production than in the 2D system [20]. In addition, the removal of RB5 increased with increasing particle electrode concentration. Activated carbon fibers [21], carbon aerogel [22], and graphite [23] have also been reported as efficient particle electrodes.

Apart from carbon-based particle electrodes, some researchers suggested metallic materials. For example, Fe particles have been successfully used as particle electrodes to treat refinery wastewater based on Fenton-like reactions [24]. The authors examined the effect of operational parameters, such as Fe dosage, and demonstrated that combining a 3D electrode and the electro Fenton system accelerate micropollutant degradation. In addition, copper ferrite ($CuFe_2O_4$) was combined with persulfate in a 3D electrode system, studying atrazine degradation [25]. Interestingly, although the examined system showed high activity towards persulfate activation, it was characterized by low adsorption capacity, especially compared to carbonaceous materials.

In order to combine the benefits of metal particles and materials of higher specific surface area, other formulations such as metal foams [26] or slags [27] were also proposed as particle electrodes. Most of these electrodes show sufficient performances, as already mentioned. However, unfortunately, it has been observed that they lose their efficiency upon repeated use, probably due to obstruction of the pores on their surface from adsorbed contaminants or leaching [19]. To overcome this drawback, catalyst-loaded particle electrodes were proposed. For example, TiO_2-SnO_2 on γ-Al_2O_3 was used as particle electrodes for chloramphenicol degradation in wastewater [28], while Bi-Sn-Sb/γ-Al_2O_3 particle electrodes showed very promising results for tetracycline removal [29].

In recent years, in the context of a holistic approach and the circular economy, the utilization of industrial by-products, such as slags [30] or minerals [31], meets higher

scientific interest for creating usable products than the use of precious raw materials. Towards this direction, biochars have piqued the scientific community's interest [32,33]. Biochars are produced from biomass residues (such as rice, oil waste, or conventional biological treatment sludge). They are a promising material for different environmental applications, such as the adsorption of organic or inorganic pollutants, improving soil quality (soil conditioner), and carbon sequestration [32,34,35]. Biochar is a carbon-rich material obtained by heating biomass at relatively moderate temperatures under limited or no atmospheric oxygen. It has been widely used as an abundant and low-cost adsorption material to remove inorganic and organic pollutants or metals from different aqueous matrices [32–34,36].

Going one step further, in their pioneering work, Fang et al. showed that in the presence of oxidants like hydrogen peroxide (but in the absence of current), biochar could act as a catalyst producing reactive oxidizing species (ROS), which can degrade organic contaminants [37]. Similar conclusions were also reported from other groups using sodium persulfate instead of hydrogen peroxide as an oxidant [38].

Based on this, the present study aims to investigate the efficiency of biochar as a particle electrode in a 3D EAOP system. For this, biochar was synthesized by calcination of sawdust under an Ar flow at different temperatures (T = 550–850 °C) and was characterized by means of BET, XRD, and SEM/EDS techniques. A BDD electrode was used as the anode electrode, and graphite as a cathode, whereas the system's efficiency was tested for the degradation of SMX, an antibiotic agent, and other emerging contaminants belonging to different groups, such as endocrine disruptors or pharmaceuticals.

As far as we know, this is the first study that examines the effect of biochar preparation conditions and the study of the observed efficiency and synergy of the hybrid process in a wide range of operating parameters, including different aqueous matrices, ions, organic loading, and environmental samples, such as bottled water and secondary effluent while at the same time the efficiency of the process was demonstrated for different micropollutants.

2. Materials and Methods

2.1. Chemicals

All the micropollutants used in this work, namely SMX, BPA, PP, and PIR, have >99% purity and were purchased from Sigma-Aldrich. Fluka supplied acetonitrile (HPLC grade) and sodium sulfate. Sodium chloride and sodium bicarbonate were also supplied by Sigma-Aldrich and used as received without any purification. Experiments were also performed using bottled water or secondary effluents, and their physicochemical characterization can be found in a previous work [39].

2.2. Preparation of Biochar

Sawdust biochar powder was obtained after calcination at different temperatures, T = 550–850 °C in Ar flow for three hours. Then, the biochar was ground in an agate mortar and used without any post-treatment. The as-prepared samples were denoted as BCS_T, where T indicates the calcination temperature.

2.3. Physicochemical Characterization Techniques

The specific surface area (SSA) of biochar was determined with the use of a micromeritics (Gemini III 2375) instrument (Norcross, GA, USA), while XRD patterns were obtained with the use of a Brucker D8 Advance instrument with a Cu Kα source (λ = 1.5496 Å). More details about the aforementioned characterization techniques can be found in former studies of our group [40,41]. SEM images were recorded on a JEOL JSM 6300 instrument (JEOL, Akishima, Tokyo, Japan), equipped with an X-ray energy dispersive spectrometer, EDS (ISIS Link 300, Oxford Instruments, High Wycombe, UK). The laser doppler micro-electrophoresis method, described by Dimitriadou et al. [42], was applied for the zeta potential measurements using a Malvern Zetasizer instrument (Malvern Instruments, Surrey, UK). Fourier transform infrared (FTIR) spectroscopy was performed using a Perkin

Elmer Spectrum, RX FTIR system (PerkinElmer Inc., Waltham, MA, USA). The measurement range was 4000–950 cm^{-1}. BCS_650 (about 0.5%) and KBr were sieved and pressured to produce a homogeneous disk.

2.4. Experimental Set-Up and Procedure

The electrochemical set-up consisted of a boron-doped diamond electrode (Adamant Technologies SA, La-Chaux-de-Fond, Switzerland; B/C 1000 ppm) serving as the anode and a graphite electrode as the cathode [43]. Their surface area was equal to 8 cm^2. The electrochemical oxidation reactor was a 150 mL square undivided cell from plexiglass, open in atmospheric conditions, and kept under magnetic stirring. The reactor was filled with 0.1 M Na_2SO_4, serving as the electrolyte containing 0.5 mg/L SMX. Experiments were conducted at 8 mA/cm^2 current density at various pH and water matrices. At pre-set periods, samples of 1.2 mL were withdrawn from the reactor, followed by the addition of 0.3 mL of methanol, filtered with 0.22 μm PVDF filters, and analyzed as follows.

2.5. Analytical Methods

The SMX concentration was measured utilizing high-performance liquid chromatography (HPLC, Waters Alliance 2695, Santa Clara, CA, USA) comprising of a photodiode array detector (Waters 2996), a gradient pump (Waters 2695), and a Kinetex column (C18 100A, 150 mm × 3 mm, 2.6 μm particle size). The system worked at 45 °C. SMX was monitored at 270 nm. BPA, PIR, and PP were detected at 230 nm, 350 nm, and 254 nm, respectively.

3. Results

Physicochemical Characterization

Notation and SSA values of various carbon-based samples are presented in Table 1. In contrast with other carbon materials, like activated carbon, the BCS was characterized by low SSA in the range of 1–3 $m^2\ g^{-1}$.

Table 1. Notation and specific surface area (SSA) values of various biochar samples.

Notation	Carbon Type	Thermal Treatment (°C)	SSA ($m^2\ g^{-1}$)
BCS_850	Biochar derived from sawdust	850	2.3 ± 0.1
BCS_750	Biochar derived from sawdust	750	3.05 ± 0.7
BCS_650	Biochar derived from sawdust	650	2.3 ± 0.3
BCS_550	Biochar derived from sawdust	550	1.1 ± 0.8

In Figure 1, the XRD patterns of the various BCS samples are presented. In the case of the BCS_650, three characteristic peaks located at 2θ = 20.72°, 21.97° and 23.43° were detected attributed to (210), (004), and (014) planes of monoclinic $C_{14}H_{13}N$ (JCPDS Card No. 34–1996), whereas the presence of the $C_{32}H_{38}N_4$ (JCPDS Card No. 13–764) was confirmed in the case of the BCS_850 and BCS_750 sample. Moreover, a peak located at 20.79° in the case of the BCS_750 XRD spectrum was attributed to $C_{12}H_{18}O_6$ (JCPDS Card No. 19–1789).

The structure and morphology of BCS_650 were further investigated by the SEM/EDS technique (Figure 2). Carbon and calcium were detected, as shown with red dots in Figure 2b,c. As demonstrated in Figure 2d, C and Ca distribution was not quite uniform. As derived from the EDS analysis (Figure 2e) the wt.% of C present in the sample was equal to ca. 27 wt.%, whereas the percentage of Ca was equal to 0.37 wt.%. The rather small percentage of Ca in the biochar structure explains its absence in the XRD spectra. The rest of the sample was oxygen (ca. 72 wt.%). The C and Ca elements were detected in the form of CO_2 and CaO, respectively. FTIR spectrum of the BCS_650 is shown in Figure S1. The peak at 3450 cm^{-1} is assigned to the stretching vibration of the –OH groups. The peaks at about 1640 and 1380 cm^{-1} correspond to C=C and C–OH groups.

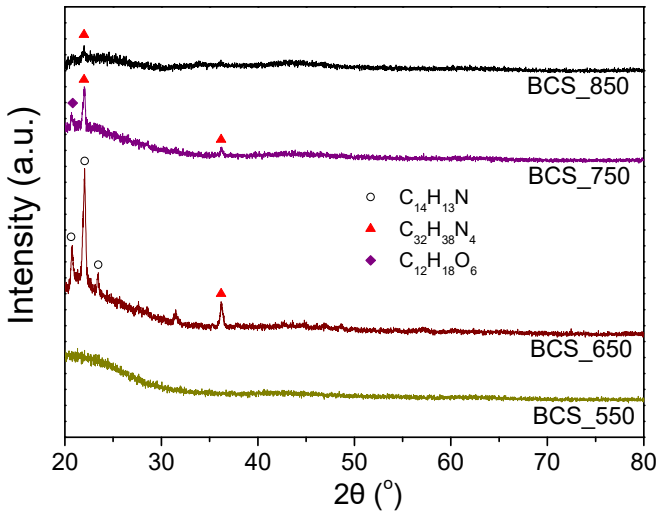

Figure 1. XRD patterns of biochar samples derived from sawdust (BCS) heat-treated at different temperatures.

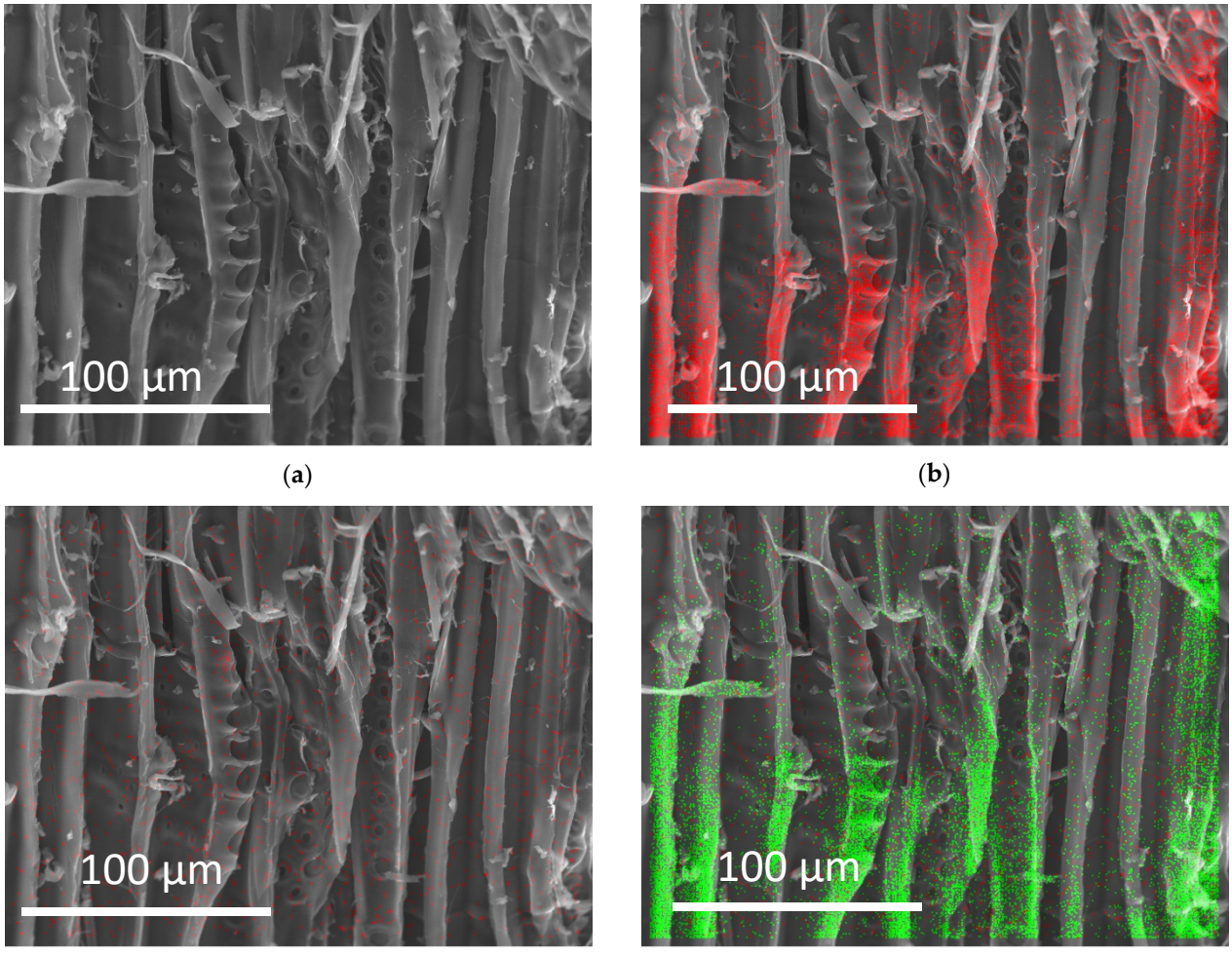

(**a**) (**b**)

(**c**) (**d**)

Figure 2. *Cont.*

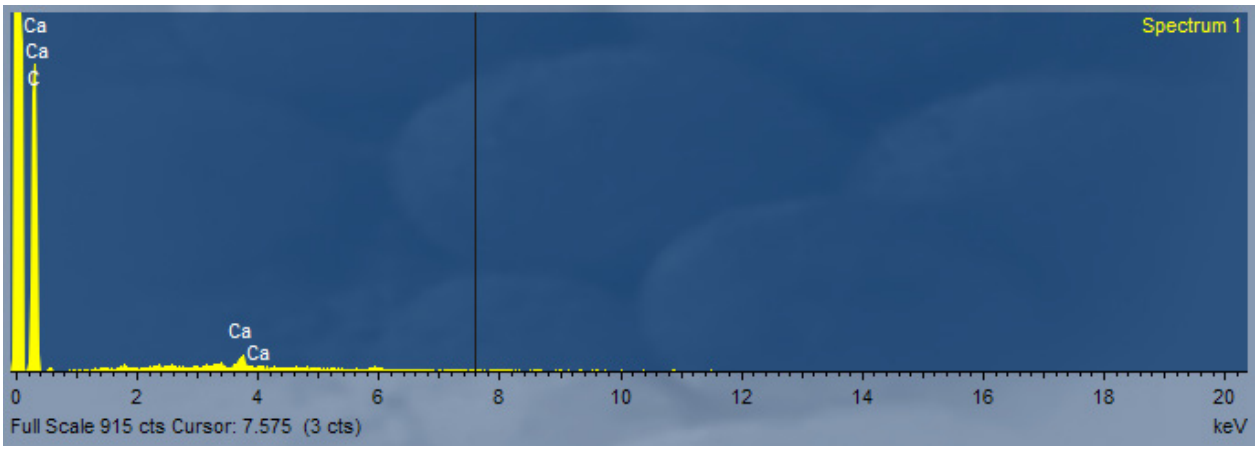

(**e**)

Figure 2. (**a**) SEM image of the BCS_650; EDS mapping results showing the distribution of (**b**) C, (**c**) Ca and (**d**) C (green spots) and Ca (red spots) elements; (**e**) corresponding EDS spectrum over the as-prepared BCS_650.

The dependence of the zeta potential values of the BSC_650 sample from the pH values is presented in Figure 3. Obviously, the BSC_650 surface is positively charged at pH < 4, whereas the higher charge value was observed at pH = 2. The zero-point charge (z.p.c.) was identified around pH = 4; while increasing the pH values, the zeta potential values decreased, implying a negative surface charge, as reported by [44,45]. The latter was also observed by other researchers [46–49]. Fahmi et al. [46] reported that the well-shaped biochar (empty fruit bunch biochar (EFBB) of oil palm) particles derived by combining the increasing adsorption capacity for Pb along with the decrease of the material particle size were the reason for the increase of the surface oxygen functional groups, thus negatively affecting the zeta potential values.

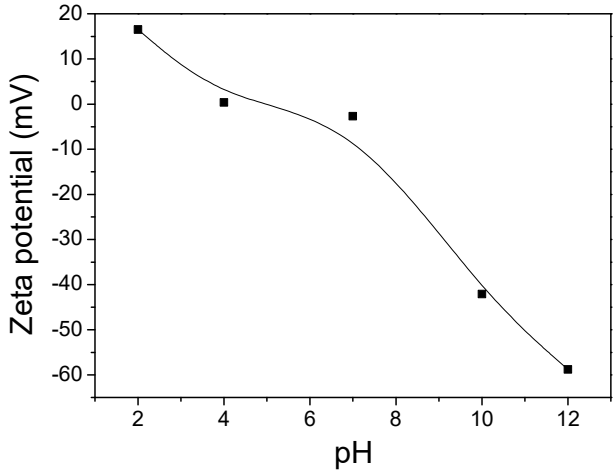

Figure 3. Zeta potential of BCS_650 as a function of pH.

Qian et al. [47] studied the aluminum-biochar interactions and highlight the amphoteric nature of biochar materials. Moreover, they correlated the observed elimination of the negative surface charge to the electrostatic attraction of Al^{3+} cations with biochar particles. The surface characteristics, as well as the porosity of biochar derived from water hyacinth plants (WH), was studied by Batista et al. [45]. Lowering the pH value resulted in an increase of the zeta potential values, as observed in the present study, which was related to the smaller ionization of the acid groups of the colloidal surface particles and/or the protonation of amine groups. Similar behavior of the zeta potential values was also

observed in the case of crop straw biochar by Yuan et al. [44] and was attributed to the charge of the colloid surface. The higher negativity of zeta potential values of the EFBB compared to that observed for the rice husks biochar (RHB) could be related to the higher adsorption of heavy metals in the case of the former, as reported by Samsuri et al. [49]. In the present study, a combination of the aforementioned reasons could be related to the increasing negative zeta potential values since formations such as $C_{14}H_{13}N$, $C_{32}H_{38}N_4$, or CaO were identified to be present on the BCS_650 structure by XRD and SEM/EDS techniques. The possible presence of Ca^+ cations could facilitate the absorption of oxygen functional groups on the biochar surface, thus negatively affecting the zeta potential values.

4. Discussion

4.1. Effect of Particle Electrode

In the first preliminary series of experiments, the effect of the synthesized biochars as particle electrodes on the destruction of 500 μg/L SMX was examined, and the results are shown in Figure 4. The experiments were performed using 0.1 M Na_2SO_4 as the electrolyte and 8 mA/cm^2 of applied current, at inherent pH with 2 g/L of biochar. As shown, the BCS_650 exhibited higher efficiency among the different biochars investigated. The apparent kinetic constants were 0.035, 0.144, 0.086 and 0.039 min^{-1} for BCS_550, BCS_650, BCS_750 and BCS_850, respectively. Taking into consideration the XRD patterns of the samples, the higher efficiency of BCS_650 is probably related to its higher crystallinity compared to the samples calcined in different temperatures. At the same time, the apparent kinetic constant for the electrooxidation over the BDD anode in the absence of biochar was 0.025 min^{-1}, resulting in only 35% SMX removal after 30 min of treatment. Therefore, the use of biochar significantly increased the removal of SMX without requiring higher applied current values, leading to a larger energy footprint and increased costs.

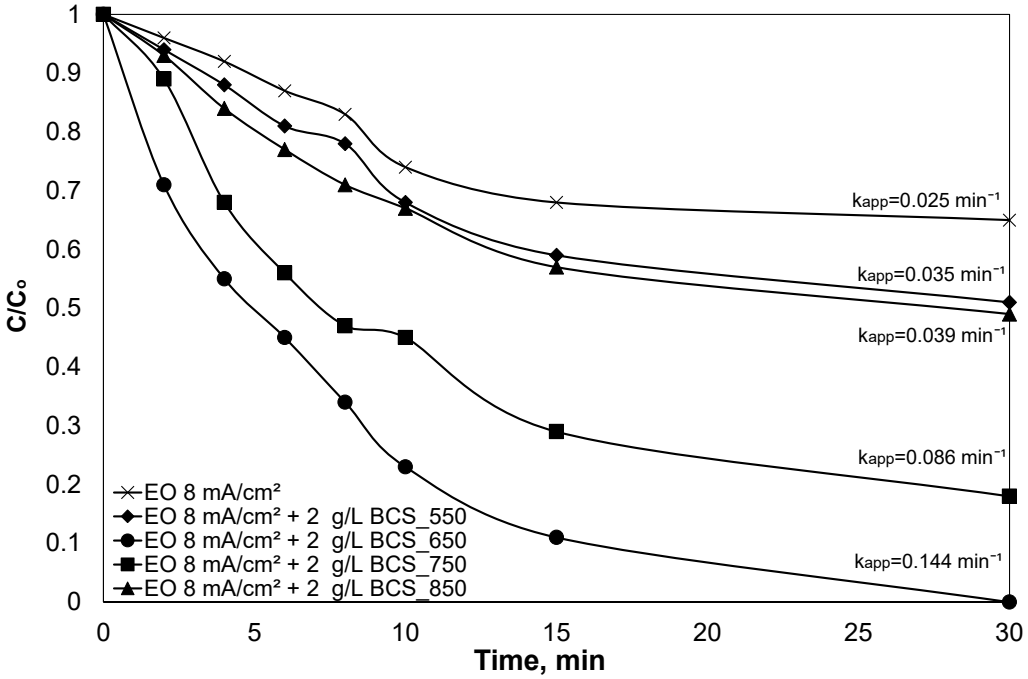

Figure 4. Effect of biochar type on the degradation of SMX in the combined 3D process. Conditions: [SMX]° = 500 μg/L, [BCS_x] = 2 g/L, [Na_2SO_4] = 0.1 M, j = 8 mA/cm^2, ultrapure water.

The biochar could interfere with the proposed system via different mechanisms.

(i) One of the first uses of biochar was as an inexpensive, environmentally friendly material for absorbing emerging contaminants. Therefore, the presence of biochar significantly increases the surface area compared to the conventional 2D electrochemical system and could provide a higher concentration of pollutants at the solid-liquid interface.

(ii) Biochars' presence increases the conductivity while the graphitic-like structure and the oxygen-containing functional groups of biochar can assist the electron transfer [50]. (iii) Depending on the origin and preparation method, biochars may have accumulated persistent free radicals on their surface. The latter could react with the absorbed organic compounds to further increase pollutants elimination [37]. (iv) Some reports have already demonstrated a biochar catalytic activity using hydrogen peroxide or persulfate as the oxidant. The latter can be produced at the anode of electrochemical systems [51], while hydrogen peroxide can be produced in electrochemical systems via oxygen reduction.

Unfortunately, the exact contribution of the different mechanisms is very difficult to quantify even with state-of-the-art equipment like Electron Paramagnetic Resonance (EPR/ESR) which was not available in the present study since the overall efficiency of the system could also involve interactions of more than one mechanism described above.

In the literature, assuming first or pseudo-first-order kinetics, the synergy index S is defined as follows [52]:

$$S = \frac{k_{combined} - {}^{n}_{i}\Sigma k_i}{k_{combined}}$$

Or in this case $S = \frac{k_{EO/BC} - k_{EO} - k_{BC}}{k_{EO/BC}}$

$$\text{where } S \begin{cases} > 0, \text{ synergistic effect} \\ = 0, \text{ cumulative effect} \\ < 0, \text{ competitive effect} \end{cases}$$

where $k_{EO/BC}$ denotes the apparent kinetic constant for the simultaneous use of electrochemical oxidation and biochar particle electrodes, k_{EO} is the apparent kinetic constant in the absence of biochar (only electrochemical oxidation) while the k_{BC} denotes the apparent kinetic constant for the pollutant adsorption on the biochar.

Substituting in the above Equation the values for the data presented in Figure 4, the degree of synergy was found equal to 0.8%, 74.5%, 55.7% and 10.3%, for BCS_550, BCS_650, BCS_750, and BCS_850, respectively, indicating that there is indeed synergy due to the presence of biochar for BCS_650 and BCS_750. At the same time, system behavior is cumulative for BCS_550 and BCS_850.

To shed light on the effect of particle electrode loading, additional experiments were conducted using 0–2 g/L of BCS_650, and the results are depicted in Figure 5. Indeed, using a higher BCS_650 loading increased the efficiency, and the observed kinetic constant as expected. The apparent kinetic constants were estimated equal to 0.025, 0.033, 0.057 and 0.144 min^{-1} for electrochemical oxidation in the presence of 0, 0.5, 1 and 2 g/L BCS_650, respectively. At the same time, the apparent kinetic constant using 2 g/L BCS_650 without applied current (i.e., adsorption) was equal to 0.012 min^{-1}. Increased biochar concentration corresponds to an increase in particulate active micro-reactors and substantially a larger surface area for the adsorption and oxidation of emerging contaminants. Furthermore, more persistent free radicals accumulated at biochars existed in the system [50,53]. In addition, the high biochar loading increases the probability of contact between biochar particle electrodes and the electrodes in the 3D electrolytic fluidized bed reactor used in this work [53].

4.2. Effect of pH

The effect of pH on the process performance was studied, and the results are shown in Figure 6. The destruction of SMX seems to be favored in near-neutral conditions. The observed kinetic constants were 0.093, 0.144, and 0.105 min^{-1} for pH 3, 6, and 10, respectively. These results are consistent with the work of Correia-Sá et al. [54] which examined the decomposition of carbamazepine into a similar 3D system consisting of activated carbon or biochar as particle electrodes and boron-doped diamond as the anode. The researchers observed that treatment efficiency was enhanced in near-neutral conditions.

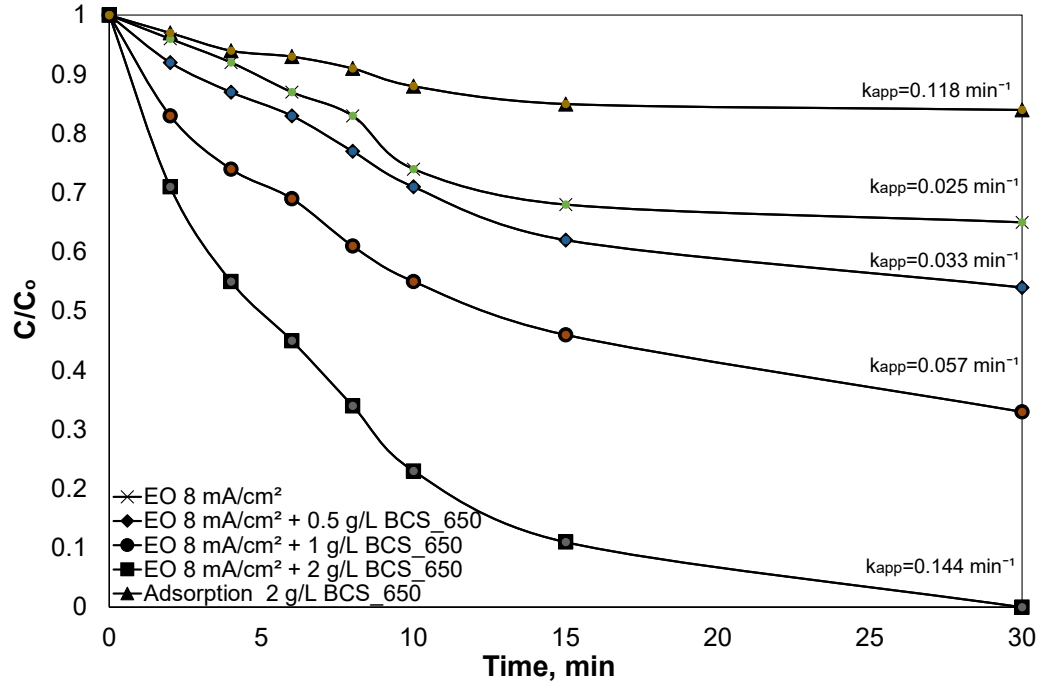

Figure 5. Effect of BCS_650 loading on the degradation of SMX in the combined 3D process. Conditions: [SMX]° = 500 μg/L, [Na_2SO_4] = 0.1 M, j = 8 mA/cm^2, ultrapure water.

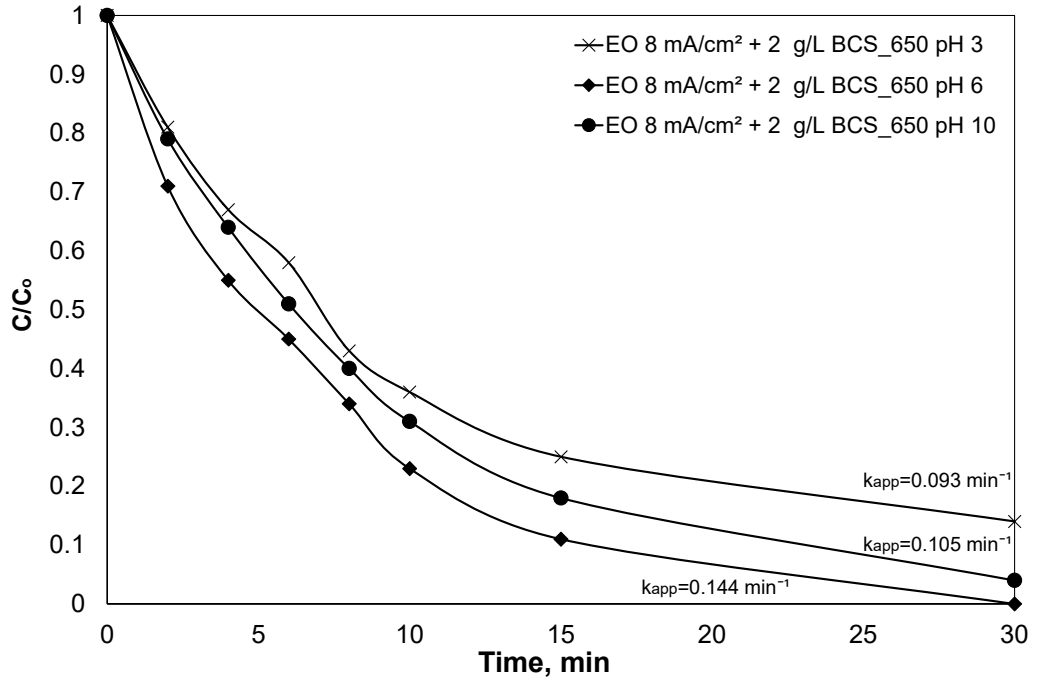

Figure 6. Effect of pH on the degradation of SMX in the combined 3D process. Conditions: [SMX]° = 500 μg/L, [BCS_650] = 2 g/L, [Na_2SO_4] = 0.1 M, j = 8 mA/cm^2, ultrapure water.

Regarding 2D electrochemical oxidation, Hai et al. [55] examined SMX electrooxidation using a boron-doped diamond anode. The oxidation favored in acidic and near-neutral conditions, and the observed kinetic constants were estimated equal to 0.067, 0.078, and 0.026 min^{-1} for pH 3, 7, and 11, respectively. The existence of an optimal pH value is justified by (a) the existence of electrostatic forces for the adsorption of pollutants in both diamond and biochar particle electrodes and (b) the different distribution and concentration of locally produced oxidizing species in different pH. At the same time, it is known that the oxidation potential of the radicals is higher in acidic conditions. It is worth noting that the

pH in most environmental systems ranges from 5.5–10. According to the results shown in Figure 6, the combined process shows satisfactory results in near-neutral conditions, which makes it advantageous over other techniques, such as the well-known Fenton reaction, which requires acidic conditions, or methods based on the activation of persulfates that usually gradually reduced the pH of the solution.

4.3. Effect of Water Matrices

One of the main problems of many physicochemical processes that act as inhibitors in their industrial application is their non-selectivity. Since, for process evaluation, most experiments are carried out in ideal laboratory conditions, the results obtained are often not representative. Therefore, it is critical to study the proposed process in real environmental systems and understand the effect of the various components of the environmental matrices. In this light, experiments were performed in the presence of inorganic ions such as bicarbonates (BIC), chlorides (Cl^-) and organic material (using humic acid (HA)) as well as in real aqueous matrices such as secondary domestic wastewater effluent (WW) and bottled water (BW), and the results are presented in Figure 7.

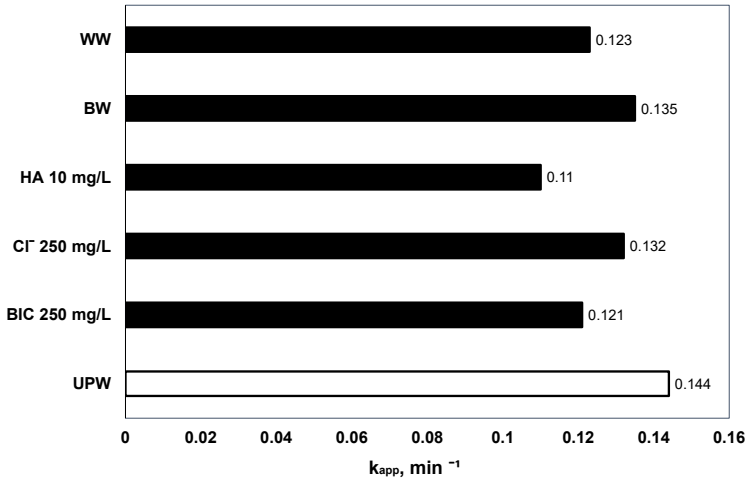

Figure 7. Effect of water matrix on the degradation of SMX in the combined 3D process. Conditions: [SMX]° = 500 μg/L, [BCS_650] = 2 g/L, [Na_2SO_4] = 0.1 M, j = 8 mA/cm^2.

It is observed that the apparent kinetic constant of the combined process decreases to a small degree in the presence of both inorganic ions and organic material, but also in the case of WW. In the case of BW, practically no reduction in a kinetic constant was shown.

The effect of aqueous matrix components is twofold: On the one hand, they compete with pollutants for adsorption on the electrode surface (but also of particulate electrodes in the combined process). On the other hand, in complex or real aqueous matrices, they react with active oxidizing species. Therefore, less than the latter are available for the desired reaction.

In several cases, the presence of chlorides can increase the electrochemical oxidation efficiency due to the formation of active chlorine, which has a longer lifespan than hydroxy radical and can diffuse into the bulk solution [14]. However, these reactions can lead to the formation of organochlorine compounds, which are highly toxic. Contrary, the proposed system did not show any increase in efficiency due to chlorides, and this may be due to (i) the system being studied in relatively mild conditions, i.e., a low applied current, and (ii) the presence of particulate electrodes decreasing the problems of the limited surface area of the electrodes that the presence of chlorine in 2D systems usually overcame.

Recently, Zhang et al. [56] investigated the adsorption of SMX using Fe-impregnated graphited biochar. The researchers did not observe any interference in the SMX adsorption in the presence of HA up to 10 mg/L. Similar results were observed for the experiments performed in river, tap, and aquaculture water.

To further test the ability of the proposed process to decompose micropollutants belonging to different chemical groups, additional experiments were performed to eliminate the endocrine disruptors BPA and PP and the nonsteroidal anti-inflammatory drug PIR. Indeed, as depicted in Figure 8, the hybrid process, as expected, degraded all the micropollutants studied in less than 45 min. The observed kinetic constants were 0.144, 0.107, 0.117, and 0.19 min^{-1} for SMX, BPA, PP, and PIR, respectively.

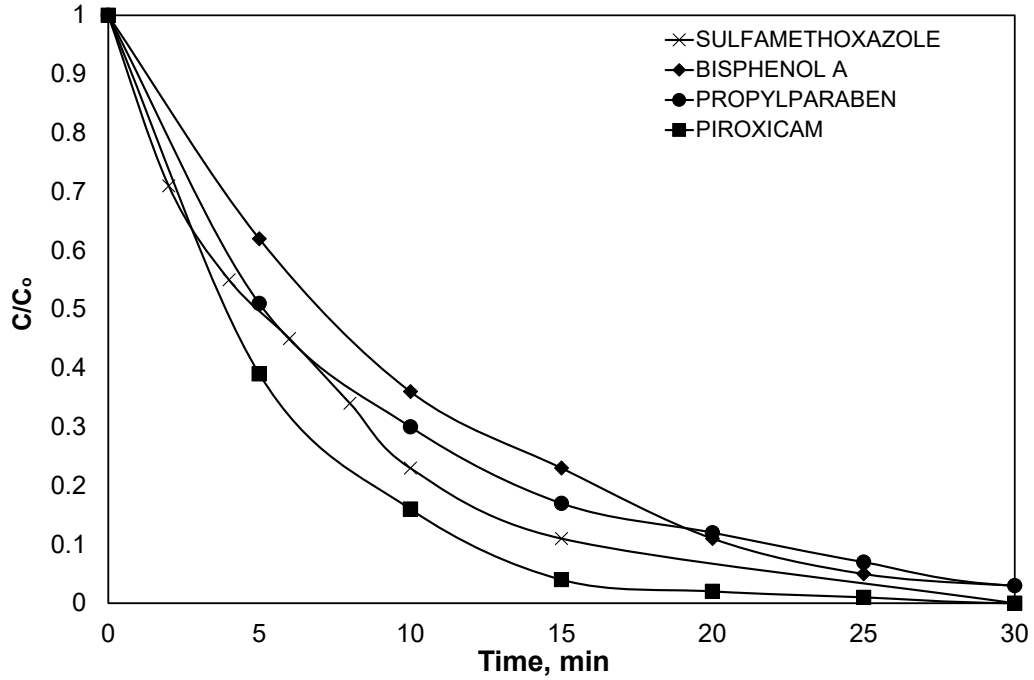

Figure 8. Degradation of different micropollutants using the hybrid 3D process. Conditions: [SMX]° = [BPA]° = [PIR]° = [PP]° = 500 μg/L, [BCS_650] = 2 g/L, [Na_2SO_4] = 0.1 M, j = 8 mA/cm^2, ultrapure water.

4.4. Biochar Reuse

In a final round of experiments, the reuse of biochar was investigated, and the results are presented in Figure 9. Interestingly the biochar retains most of its ability since the apparent kinetic constant was decreased almost 23%, from 0.144 to 0.112 min^{-1} after five sequential experiments. It is worth noting that most of this drop (18%) takes place after the first experiment, while the system shows satisfactory stability in the remaining experiments.

After all, the ability to reuse biochar distinguishes this combined process from the sequentation of electrochemical oxidation with adsorption in series. In this case, the efficiency will decrease rapidly as soon as the saturation of the adsorbent material occurs. Despite the encouraging retention of efficiency, these results must be addressed with caution since they represented a snapshot of the proposed system under specific conditions. Therefore, in future work, a detailed examination of the stability of the particle electrodes is needed and the operation under a continuous flow mode is suggested. In addition, particular emphasis must be given to the examination of different possibilities for the regeneration of the biochar that was outside of the scope of the current work.

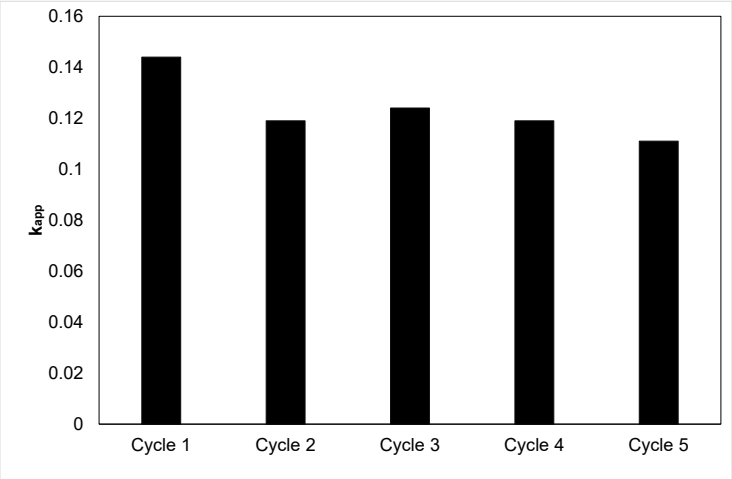

Figure 9. Effect of biochar reuse on the degradation of SMX in the combined 3D process. Conditions: [SMX]° = 500 μg/L, [BCS_650] = 2 g/L, [Na_2SO_4] = 0.1 M, j = 8 mA/cm^2, ultrapure water.

5. Conclusions and Future Perspectives

In this work, a hybrid electrochemical system based on biochar was tested to eliminate emerging contaminants from the aqueous phase. The proposed system gave promising results for different micropollutants. In conclusion, the use of agro-industrial by-products such as biochars can be an interesting alternative for replacing known materials such as activated carbon. Of particular interest is that the proposed combination retains its high efficiency in experiments performed in complex aqueous matrices, unlike other well-known physicochemical processes. At the same time, the biochar used as a particle electrode can be reused without a significant drop in efficiency, at least in the range of the conditions studied.

Although the results are promising, future work in different directions is needed to understand the mechanism of the proposed system. Therefore, future research needs to be directed towards (i) a thorough examination of the stability of the particle electrodes through the reuse and regeneration of biochar under different conditions, (ii) a correlation between the raw precursor biochar, the physicochemical characteristics, and the efficiency of the hybrid process, (iii) the examination of the contribution of different mechanisms on the observed efficiency. Conventional direct and indirect electrochemical oxidation have proven its potential as a disinfection process. Therefore, future research and applications of the proposed process involve the simultaneous degradation of micropollutants, removal of natural or effluent organic matter, and disinfection since the final goal is to examine whether the proposed process can be used as a complete and environmentally friendly solution for tertiary wastewater treatment.

Supplementary Materials: The following supporting information can be downloaded at: https://www.mdpi.com/article/10.3390/w14030357/s1, Figure S1: FTIR spectrum of the BCS_650.

Author Contributions: Conceptualization, Z.F. and A.P.; methodology, Z.F., A.P. and G.B.; investigation, Z.F., A.P. and G.B.; writing—original draft preparation, Z.F., A.P. and G.B.; writing—review and editing, Z.F., A.P. and G.B.; supervision, Z.F. and A.P.; project administration, Z.F. and A.P. All authors have read and agreed to the published version of the manuscript.

Funding: This research is co-financed by Greece and the European Union (European Social Fund—ESF) through the Operational Program Human Resources Development, Education and Lifelong Learning 2014–2020 in the context of the project development of an innovative biomass-based hybrid electrochemical process for the removal of endocrine disruptors (MIS 5050535).

Institutional Review Board Statement: Not applicable.

Informed Consent Statement: Not applicable.

Acknowledgments: SEM and EDS measurements were performed by Katerina Govatsi at the Laboratory of Electron Microscopy and Microanalysis (L.E.M.M.) of the University of Patras, Greece. This contribution is gratefully acknowledged.

Conflicts of Interest: The authors declare no conflict of interest.

References

1. Kanakaraju, D.; Glass, B.D.; Oelgemöller, M. Advanced oxidation process-mediated removal of pharmaceuticals from water: A review. *J. Environ. Manag.* **2018**, *219*, 189–207. [CrossRef] [PubMed]
2. Olasupo, A.; Suah, F.B.M. Recent advances in the removal of pharmaceuticals and endocrine-disrupting compounds in the aquatic system: A case of polymer inclusion membranes. *J. Hazard. Mater.* **2021**, *406*, 124317. [CrossRef] [PubMed]
3. Vilela, C.L.S.; Bassin, J.P.; Peixoto, R.S. Water contamination by endocrine disruptors: Impacts, microbiological aspects and trends for environmental protection. *Environ. Pollut.* **2018**, *235*, 546–559. [CrossRef] [PubMed]
4. Gonsioroski, A.; Mourikes, V.E.; Flaws, J.A. Endocrine Disruptors in Water and Their Effects on the Reproductive System. *Int. J. Mol. Sci.* **2020**, *21*, 1929. [CrossRef] [PubMed]
5. Giannakis, S.; Lin, K.-Y.A.; Ghanbari, F. A review of the recent advances on the treatment of industrial wastewaters by Sulfate Radical-based Advanced Oxidation Processes (SR-AOPs). *Chem. Eng. J.* **2021**, *406*, 127083. [CrossRef]
6. García-Espinoza, J.D.; Nacheva, P.M. Degradation of pharmaceutical compounds in water by oxygenated electrochemical oxidation: Parametric optimization, kinetic studies and toxicity assessment. *Sci. Total Environ.* **2019**, *691*, 417–429. [CrossRef] [PubMed]
7. Herraiz-Carboné, M.; Cotillas, S.; Lacasa, E.; Moratalla, Á.; Cañizares, P.; Rodrigo, M.A.; Sáez, C. Improving the biodegradability of hospital urines polluted with chloramphenicol by the application of electrochemical oxidation. *Sci. Total Environ.* **2020**, *725*, 138430. [CrossRef]
8. Brillas, E.; Martínez-Huitle, C.A. Decontamination of wastewaters containing synthetic organic dyes by electrochemical methods. An updated review. *Appl. Catal. B Environ.* **2015**, *166–167*, 603–643. [CrossRef]
9. Cotillas, S.; Llanos, J.; Cañizares, P.; Clematis, D.; Cerisola, G.; Rodrigo, M.A.; Panizza, M. Removal of Procion Red MX-5B dye from wastewater by conductive-diamond electrochemical oxidation. *Electrochim. Acta* **2018**, *263*, 1–7. [CrossRef]
10. Ganiyu, S.O.; Oturan, N.; Raffy, S.; Cretin, M.; Causserand, C.; Oturan, M.A. Efficiency of plasma elaborated sub-stoichiometric titanium oxide (Ti_4O_7) ceramic electrode for advanced electrochemical degradation of paracetamol in different electrolyte media. *Sep. Purif. Technol.* **2019**, *208*, 142–152. [CrossRef]
11. Särkkä, H.; Bhatnagar, A.; Sillanpää, M. Recent developments of electrooxidation in water treatment—A review. *J. Electroanal. Chem.* **2015**, *754*, 46–56. [CrossRef]
12. Radjenovic, J.; Sedlak, D.L. Challenges and Opportunities for Electrochemical Processes as Next-Generation Technologies for the Treatment of Contaminated Water. *Environ. Sci. Technol.* **2015**, *49*, 11292–11302. [CrossRef] [PubMed]
13. Sun, W.; Sun, Y.; Shah, K.J.; Zheng, H.; Ma, B. Electrochemical degradation of oxytetracycline by Ti-Sn-Sb/γ-Al_2O_3 three-dimensional electrodes. *J. Environ. Manag.* **2019**, *241*, 22–31. [CrossRef] [PubMed]
14. Bampos, G.; Petala, A.; Frontistis, Z. Recent Trends in Pharmaceuticals Removal from Water Using Electrochemical Oxidation Processes. *Environments* **2021**, *8*, 85. [CrossRef]
15. Zhang, T.; Zhu, H.; Croué, J.-P. Production of Sulfate Radical from Peroxymonosulfate Induced by a Magnetically Separable $CuFe_2O_4$ Spinel in Water: Efficiency, Stability, and Mechanism. *Environ. Sci. Technol.* **2013**, *47*, 2784–2791. [CrossRef]
16. Pan, G.; Jing, X.; Ding, X.; Shen, Y.; Xu, S.; Miao, W. Synergistic effects of photocatalytic and electrocatalytic oxidation based on a three-dimensional electrode reactor toward degradation of dyes in wastewater. *J. Alloys Compd.* **2019**, *809*, 151749. [CrossRef]
17. Shen, B.; Wen, X.; Huang, X. Enhanced removal performance of estriol by a three-dimensional electrode reactor. *Chem. Eng. J.* **2017**, *327*, 597–607. [CrossRef]
18. Ji, J.; Li, X.; Xu, J.; Yang, X.; Meng, H.; Yan, Z. Zn-Fe-rich granular sludge carbon (GSC) for enhanced electrocatalytic removal of bisphenol A (BPA) and Rhodamine B (RhB) in a continuous-flow three-dimensional electrode reactor (3DER). *Electrochim. Acta* **2018**, *284*, 587–596. [CrossRef]
19. Zhan, J.; Li, Z.; Yu, G.; Pan, X.; Wang, J.; Zhu, W.; Han, X.; Wang, Y. Enhanced treatment of pharmaceutical wastewater by combining three-dimensional electrochemical process with ozonation to in situ regenerate granular activated carbon particle electrodes. *Sep. Purif. Technol.* **2019**, *208*, 12–18. [CrossRef]
20. Nezamaddin, M.; Hamidreza, P.; Khodadadi, S.M.; Yaghoub, H.; Iman, P.; Saeed, P.; Noureddin, N. Electrochemical Degradation of Reactive Black 5 Using Three-Dimensional Electrochemical System Based on Multiwalled Carbon Nanotubes. *J. Environ. Eng.* **2019**, *145*, 4019021. [CrossRef]
21. Hassan, M.F.; Sabri, M.A.; Fazal, H.; Hafeez, A.; Shezad, N.; Hussain, M. Recent trends in activated carbon fibers production from various precursors and applications—A comparative review. *J. Anal. Appl. Pyrolysis* **2020**, *145*, 104715. [CrossRef]
22. Cao, Z.; Zhang, C.; Yang, Z.; Qin, Q.; Zhang, Z.; Wang, X.; Shen, J. Preparation of Carbon Aerogel Electrode for Electrosorption of Copper Ions in Aqueous Solution. *Materials* **2019**, *12*, 1864. [CrossRef] [PubMed]

23. Huang, T.; Zhang, S.; Liu, L.; Xu, J. Graphite particle electrodes that enhance the detoxification of municipal solid waste incineration fly ashes in a three-dimensional electrokinetic platform and its mechanisms. *Environ. Pollut.* **2018**, *243*, 929–939. [CrossRef] [PubMed]
24. Yan, L.; Wang, Y.; Li, J.; Shen, H.; Zhang, C.; Qu, T. Reduction of Chemical Oxygen Demand from Refinery Wastewater by Three-Dimensional Electrode-Electro-Fenton Process. *Bull. Chem. Soc. Jpn.* **2015**, *89*, 50–57. [CrossRef]
25. Li, J.; Yan, J.; Yao, G.; Zhang, Y.; Li, X.; Lai, B. Improving the degradation of atrazine in the three-dimensional (3D) electrochemical process using CuFe2O4 as both particle electrode and catalyst for persulfate activation. *Chem. Eng. J.* **2019**, *361*, 1317–1332. [CrossRef]
26. Chaudhari, N.K.; Jin, H.; Kim, B.; Lee, K. Nanostructured materials on 3D nickel foam as electrocatalysts for water splitting. *Nanoscale* **2017**, *9*, 12231–12247. [CrossRef]
27. Liu, S.; Wang, Z.; Li, J.; Zhao, C.; He, X.; Yang, G. Fabrication of slag particle three-dimensional electrode system for methylene blue degradation: Characterization, performance and mechanism study. *Chemosphere* **2018**, *213*, 377–383. [CrossRef]
28. Sun, Y.; Li, P.; Zheng, H.; Zhao, C.; Xiao, X.; Xu, Y.; Sun, W.; Wu, H.; Ren, M. Electrochemical treatment of chloramphenicol using Ti-Sn/γ-Al_2O_3 particle electrodes with a three-dimensional reactor. *Chem. Eng. J.* **2017**, *308*, 1233–1242. [CrossRef]
29. Sun, W.; Sun, Y.; Shah, K.J.; Chiang, P.-C.; Zheng, H. Electrocatalytic oxidation of tetracycline by Bi-Sn-Sb/γ-Al_2O_3 three-dimensional particle electrode. *J. Hazard. Mater.* **2019**, *370*, 24–32. [CrossRef]
30. Habib, A.; Bhatti, H.N.; Iqbal, M. Metallurgical Processing Strategies for Metals Recovery from Industrial Slags. *Z. Phys. Chem.* **2020**, *234*, 201–231. [CrossRef]
31. Hong, L.; Yang, Q.; Liying, Z.; Yingyan, C.; Bing, W. Investigation of a novel pyrolusite particle electrode effects in the chlorine-containing wastewater. *Water Sci. Technol.* **2018**, *78*, 1427–1437. [CrossRef] [PubMed]
32. Ahmad, M.; Rajapaksha, A.U.; Lim, J.E.; Zhang, M.; Bolan, N.; Mohan, D.; Vithanage, M.; Lee, S.S.; Ok, Y.S. Biochar as a sorbent for contaminant management in soil and water: A review. *Chemosphere* **2014**, *99*, 19–33. [CrossRef] [PubMed]
33. Brown, R. Biochar Production Technology. In *Biochar for Environmental Management: Science and Technology*; Routledge: Abingdon, UK, 2012; ISBN 9781849770552.
34. Mohan, D.; Sarswat, A.; Ok, Y.S.; Pittman, C.U. Organic and inorganic contaminants removal from water with biochar, a renewable, low cost and sustainable adsorbent—A critical review. *Bioresour. Technol.* **2014**, *160*, 191–202. [CrossRef] [PubMed]
35. Lehmann, J.; Joseph, S. *Biochar for Environmental Management: Science, Technology and Implementation*; Routledge: Abingdon, UK, 2021; ISBN 9780367779184-0367779188.
36. Chen, B.; Chen, Z.; Lv, S. A novel magnetic biochar efficiently sorbs organic pollutants and phosphate. *Bioresour. Technol.* **2011**, *102*, 716–723. [CrossRef] [PubMed]
37. Fang, G.; Gao, J.; Liu, C.; Dionysiou, D.D.; Wang, Y.; Zhou, D. Key Role of Persistent Free Radicals in Hydrogen Peroxide Activation by Biochar: Implications to Organic Contaminant Degradation. *Environ. Sci. Technol.* **2014**, *48*, 1902–1910. [CrossRef] [PubMed]
38. Kemmou, L.; Frontistis, Z.; Vakros, J.; Manariotis, I.D.; Mantzavinos, D. Degradation of antibiotic sulfamethoxazole by biochar-activated persulfate: Factors affecting the activation and degradation processes. *Catal. Today* **2018**, *313*, 128–133. [CrossRef]
39. Ioannidi, A.; Arvaniti, O.S.; Nika, M.C.; Aalizadeh, R.; Thomaidis, N.S.; Mantzavinos, D.; Frontistis, Z. Removal of drug losartan in environmental aquatic matrices by heat-activated persulfate: Kinetics, transformation products and synergistic effects. *Chemosphere* **2022**, *287*, 131952. [CrossRef]
40. Arvaniti, O.S.; Petala, A.; Zalaora, A.A.; Mantzavinos, D.; Frontistis, Z. Solar light-induced photocatalytic degradation of methylparaben by g-C_3N_4 in different water matrices. *J. Chem. Technol. Biotechnol.* **2020**, *95*, 2811–2821. [CrossRef]
41. Petala, A.; Tsikritzis, D.; Kollia, M.; Ladas, S.; Kennou, S.; DI, K. Synthesis and characterization of N-doped TiO_2 photocatalysts with tunable response to solar radiation. *Appl. Surf. Sci.* **2014**, *305*, 281–291. [CrossRef]
42. Dimitriadou, S.; Frontistis, Z.; Petala, A.; Bampos, G.; Mantzavinos, D. Carbocatalytic activation of persulfate for the removal of drug diclofenac from aqueous matrices. *Catal. Today* **2020**, *355*, 937–944. [CrossRef]
43. Kouskouki, A.; Chatzisymeon, E.; Mantzavinos, D.; Frontistis, Z. Electrochemical Degradation of Piroxicam on a Boron-Doped Diamond Anode: Investigation of Operating Parameters and Ultrasound Synergy. *ChemElectroChem* **2019**, *6*, 841–847. [CrossRef]
44. Yuan, J.-H.; Xu, R.-K. The amelioration effects of low temperature biochar generated from nine crop residues on an acidic Ultisol. *Soil Use Manag.* **2011**, *27*, 110–115. [CrossRef]
45. Batista, E.M.C.C.; Shultz, J.; Matos, T.T.S.; Fornari, M.R.; Ferreira, T.M.; Szpoganicz, B.; de Freitas, R.A.; Mangrich, A.S. Effect of surface and porosity of biochar on water holding capacity aiming indirectly at preservation of the Amazon biome. *Sci. Rep.* **2018**, *8*, 10677. [CrossRef] [PubMed]
46. Fahmi, A.H.; Samsuri, A.W.; Jol, H.; Singh, D. Physical modification of biochar to expose the inner pores and their functional groups to enhance lead adsorption. *RSC Adv.* **2018**, *8*, 38270–38280. [CrossRef]
47. Qian, L.; Chen, B. Interactions of Aluminum with Biochars and Oxidized Biochars: Implications for the Biochar Aging Process. *J. Agric. Food Chem.* **2014**, *62*, 373–380. [CrossRef] [PubMed]
48. Mukherjee, A.; Zimmerman, A.R.; Harris, W. Surface chemistry variations among a series of laboratory-produced biochars. *Geoderma* **2011**, *163*, 247–255. [CrossRef]
49. Samsuri, A.W.; Sadegh-Zadeh, F.; Seh-Bardan, B.J. Characterization of biochars produced from oil palm and rice husks and their adsorption capacities for heavy metals. *Int. J. Environ. Sci. Technol.* **2014**, *11*, 967–976. [CrossRef]

50. Liu, Q.; Bai, X.; Su, X.; Huang, B.; Wang, B.; Zhang, X.; Ruan, X.; Cao, W.; Xu, Y.; Qian, G. The promotion effect of biochar on electrochemical degradation of nitrobenzene. *J. Clean. Prod.* **2020**, *244*, 118890. [CrossRef]
51. Frontistis, Z.; Mantzavinos, D.; Meriç, S. Degradation of antibiotic ampicillin on boron-doped diamond anode using the combined electrochemical oxidation—Sodium persulfate process. *J. Environ. Manag.* **2018**, *223*, 878–887. [CrossRef]
52. Stathoulopoulos, A.; Mantzavinos, D.; Frontistis, Z. Coupling Persulfate-Based AOPs: A Novel Approach for Piroxicam Degradation in Aqueous Matrices. *Water* **2020**, *12*, 1530. [CrossRef]
53. Li, H.; Yang, H.; Cheng, J.; Hu, C.; Yang, Z.; Wu, C. Three-dimensional particle electrode system treatment of organic wastewater: A general review based on patents. *J. Clean. Prod.* **2021**, *308*, 127324. [CrossRef]
54. Correia-sá, L.; Soares, C.; Freitas, O.M.; Moreira, M.M.; Nouws, H.P.A.; Correia, M.; Paíga, P.; Rodrigues, A.J.; Oliveira, C.M.; Figueiredo, S.A.; et al. A three-dimensional electrochemical process for the removal of carbamazepine. *Appl. Sci.* **2021**, *11*, 6432. [CrossRef]
55. Hai, H.; Xing, X.; Li, S.; Xia, S.; Xia, J. Electrochemical oxidation of sulfamethoxazole in BDD anode system: Degradation kinetics, mechanisms and toxicity evaluation. *Sci. Total Environ.* **2020**, *738*, 139909. [CrossRef] [PubMed]
56. Zhang, R.; Zheng, X.; Chen, B.; Ma, J.; Niu, X.; Zhang, D.; Lin, Z.; Fu, M.; Zhou, S. Enhanced adsorption of sulfamethoxazole from aqueous solution by Fe-impregnated graphited biochar. *J. Clean. Prod.* **2020**, *256*, 120662. [CrossRef]